Encyclopedia of Computational Neuroscience
DOI 10.1007/978-1-4614-7320-6_603-6

Paraspinal Magnetic and Transcutaneous Electrical Stimulation

Ursula S. Hofstoetter*, Simon M. Danner and Karen Minassian
Center of Medical Physics and Biomedical Engineering, Medical University of Vienna, Institute of Analysis and Scientific Computing, Vienna University of Technology, Vienna, Austria

Synonyms

High-voltage paraspinal electrical stimulation; High-voltage percutaneous electrical stimulation; Magnetic paravertebral stimulation; Magnetic spinal stimulation; Paravertebral neuromagnetic stimulation; Spinal electromagnetic stimulation; Spinal neuromagnetic stimulation; Spinal root stimulation; Transcutaneous posterior root stimulation; Transcutaneous spinal cord stimulation; Transcutaneous spinal stimulation; Transspinal stimulation

Definition

Paraspinal magnetic and electrical stimulation target deep neural structures within the vertebral canal and in between neighboring vertebrae from a distance of several centimeters, with either magnetic coils or skin electrodes. The principal mechanism of stimulation at the neuronal level is the same for magnetic and electrical stimulation and is given by the induced electric field component or, in an equivalent way, the electric potential, generated along the anatomical path of the nerve fibers. Yet the generation of electric fields by electromagnetic induction or electrical stimulation bases on different physical principles, and the currents generated differ substantially, both as a function of time (pulse shape) and space (distribution in the body tissues). Induced ionic tissue currents secondary to externally applied, time-varying magnetic fields enter the spine predominantly from its sides, while the currents generated by transcutaneous electrical stimulation penetrate it mainly from its back (or front). The motor fibers within the spinal nerves and anterior rootlets are the common targets of paraspinal magnetic stimulation. Different techniques of transcutaneous electrical stimulation either excite the motor fibers in the spinal nerves/anterior rootlets or selectively activate the sensory fibers within the posterior roots/rootlets. Furthermore, longitudinal tracts within the white matter of the spinal cord can be directly activated by high-voltage electrical stimulation. Neural networks of the spinal cord gray matter are exclusively activated transsynaptically, e.g., through the inputs provided by electrically stimulated sensory fibers. The applications of paraspinal magnetic and transcutaneous electrical stimulation depend on the stimulated neuroanatomy. They include the neurodiagnostic assessment of the functional integrity of lower motoneurons, neurophysiological studies of spinal cord neural networks, the generation of patterned muscle contractions for useful bodily functions, and neuromodulation applications.

*Email: ursula.hofstoetter@meduniwien.ac.at

Encyclopedia of Computational Neuroscience
DOI 10.1007/978-1-4614-7320-6_603-6

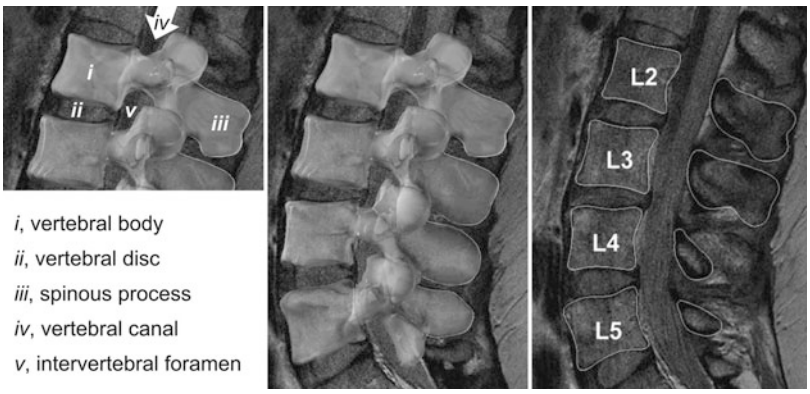

Fig. 1 Geometry of the human spine. Three-dimensional representation of the human lumbar spine (second to fifth lumbar vertebrae) constructed using magnetic resonance (*MR*) images and an MR image in sagittal plane. While the bony structures appear quite massive in the three-dimensional representation, the section shows the extent of soft tissues with better electrical conductivities. The anterior to posterior direction is from left to right (Reproduced from Xia et al. (2009) with permission from Springer Science and Business Media)

Detailed Description

Magnetic and transcutaneous electrical stimulation applied over the spine and spinal cord produce electric fields by different physical principles. Paraspinal magnetic stimulation generates continuous, ionic current flows that close on themselves following the principles of electromagnetic induction. The current flow is largely constrained to planes parallel to the surface of the volume conductor in contact with the magnetic coil, i.e., to the back. Hence, the induced currents are mainly circular and oriented parallel to the frontal (coronal) plane. In transcutaneous electrical stimulation, the potential difference between the skin electrodes during a stimulation pulse causes current to flow from the anode to the cathode via the intermediate anatomical structures. Close to the paraspinal electrodes and also within the spine, current flows have directions perpendicular to the frontal plane. The current flows generated by paraspinal magnetic and electrical stimulation are thus very unalike.

Within the human body, the current flow is shaped by the electrical tissue properties and the numerous conductivity boundaries. The bony structures of the spine, owing to their high electrical resistance, have a considerable influence on the produced currents. Yet, unlike the brain, the spinal roots and spinal cord are not completely enclosed by bony material. The electrical resistance across the spine is reduced by soft tissues, including ligaments and disks, between neighboring vertebrae (Fig. 1). Structures within the "openings" of the spine have better electrical conductivities than the bones as well. The longitudinal, centrally located vertebral canal contains the spinal cord and spinal roots. It is formed by the vertebrae and, in the intervertebral spaces, by the ligaments. The intervertebral foramina (or neuroforamina) are the bilateral openings between every pair of vertebrae that allow for the exits of the spinal roots/nerves from the vertebral canal. The sacral canal is the continuation of the vertebral canal within the sacral bone of the pelvis. Its openings for the sacral roots of the cauda equina, the anterior sacral foramina, have a posteroanterior orientation.

A further important influence on the immediate stimulation effects is given by the fiber paths of the neural target structures, i.e., the alterations of their spatial orientation with respect to the electric field. Cervical and upper thoracic roots course laterally or slightly downward from the spinal cord to the respective intervertebral foramina. There, they have short, upwardly directed segments. Lumbar and sacral roots have a sharp, caudally directed bend as they exit the spinal cord, followed by a longitudinal component through the cauda equina. The roots then exit the canal at angles between

DOI 10.1007/978-1-4614-7320-6_603-6

20° and 40° to the longitudinal axis, with a rather mediolateral orientation at the intervertebral foramina and a posteroanterior orientation at the anterior sacral neuroforamina.

General Principles of Nerve Stimulation

The substructure of a neuron most excitable by external stimulation is the myelinated axon. In magnetic stimulation, the activation of the axon is not directly caused by the magnetic field but by the electromagnetically induced electric field. The principal mechanism of neural stimulation is thus the same for paraspinal magnetic and electrical stimulation. The electric field $\mathbf{E}$ is a vector field given in V/m. Equally, the electric potential Φ, a scalar field measured in V, describes the stimulation effects upon the neural structures. Their relation is given by $\mathbf{E} = -\nabla\Phi$. The stimulation-generated electric field/potential distribution causes ionic currents to flow within the electrically conducting anatomical structures. A fraction of the current passes the nerve fiber membranes, thereby producing local depolarizations and hyperpolarizations. Depolarization of the membrane to a threshold level generates an action potential that normally propagates in both directions along the nerve fiber. Low excitation thresholds result from sudden changes of the electric field component or of the potential distribution along the axon's anatomical path. More precisely, the strongest depolarization is produced at the peak of the second-order spatial difference of the electric potential along the nerve fiber (Rattay 1999 and see entry ▶ Finite Element Modeling for Extracellular Stimulation). Equivalently, the depolarization is proportional to the negative-going, first-order spatial difference of the electric field tangential to the fiber path. Effective stimulation of a large-diameter myelinated axon requires changes of the electric potential across distances covering neighboring nodes of Ranvier, i.e., distances of few millimeters. Along such distances, large values of the second-order spatial difference of the electric potential can be present even in a non-focal electric field, if an axon (i) alters its spatial orientation within the field or (ii) passes electrical inhomogeneities of the tissues surrounding it. Considerable inhomogeneities arise across the intervertebral foramina, as well as at the interface between the spinal rootlets and the spinal cord (sudden change in conductance between the cerebrospinal fluid and the spinal cord). At the same sites, these inhomogeneities are added to by the alterations of the spatial orientation of the sensory and motor fibers, particularly those of the lumbar and sacral roots. Due to these low-threshold sites, deep neural structures can be stimulated, and the depolarization sites are predictable in spite of the distant stimulation and widespread fields.

Biophysics of Paraspinal Magnetic and Transcutaneous Electrical Stimulation

Paraspinal Magnetic Stimulation

Magnetic stimulation follows the fundamental principles of electromagnetic induction. A brief electric current pulse flowing in a coil of wires creates a time-varying magnetic field. The magnetic field passes unimpeded through biological tissues with low electrical conductivity and gives rise to an electric field. Within the electrically conductive tissues of the human body, the electric field causes ionic current flows. These induced secondary currents are circular, flowing in the opposite direction to the primary coil current, and are affected by the inhomogeneous and anisotropic electrical tissue properties. A principal difference between magnetic and transcutaneous electrical stimulation in the activation of deep neural structures is that these secondary currents do not flow from the body surface to the target but are induced without localized electrical "sources" or "sinks"

DOI 10.1007/978-1-4614-7320-6_603-6

within the body volume. The relatively low current densities at the skin below the coil result in a reduced excitation of nerve endings that may otherwise cause discomfort.

The magnetic field (i.e., the magnetic flux density **B**) is a vector field given in tesla (1 T = 1 Vs/m^2). The magnetic field lines are closed loops, cross the coil plane at perpendicular angles, and curve outward from the coil. At the center of a round coil, maximum magnetic fields of 1–2.5 T are generated. The effective depth of magnetic stimulation is limited by the rapid (exponential) decay of the induced electric field along a line perpendicular to the coil's plane. As a function of time, the magnetic field exhibits the same waveform as the coil current. The current waveform and the current direction within the coil are thus critical electrical characteristics determining the stimulation effects. Monophasic (or near-monophasic) and biphasic (or damped oscillatory) waveforms are produced by conventional magnetic stimulators, usually with rise times of 50–200 μs and durations of 100–1,000 μs. The monophasic coil current waveform has a rapid rise time and a slower decay to zero. The current producing the magnetic field flows in one direction of the coil only. Thus, by flipping the coil, the direction of the secondary currents induced in the human tissues is reversed, which generally has an influence on the thresholds of the neural target structures. The waveform of a biphasic coil current pulse is a decaying full cycle of a sine wave (Fig. 2a, dotted line). With the secondary currents induced in either direction, the determination of the site of stimulation may become more difficult.

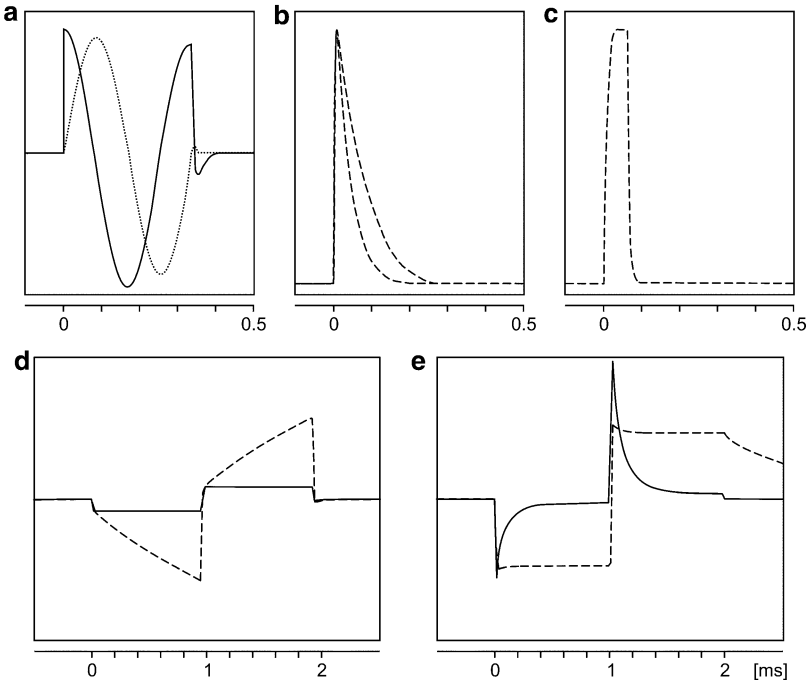

Fig. 2 Pulse shapes of paraspinal magnetic and electrical stimulation. (**a**) Biphasic pulse of a magnetic stimulator; the *dotted line* is the basic waveform of the coil current and the magnetic flux density and the *solid line* is that of the induced electric field and secondary tissue current. (**b**, **c**) show the voltage across a resistor produced by the Digitimer D180 (decay constant set at 50 and 100 μs) and the Digitimer D185, respectively, both applied in high-voltage electrical stimulation. (**d**, **e**) are the biphasic pulses of a current-controlled and a voltage-controlled stimulator, respectively, as used for transcutaneous spinal cord stimulation. *Solid lines* are currents through and *dashed lines* are voltages across an individual, measured at the electrodes during stimulation. The scaling of the ordinates is arbitrary; the figures compare the stimulation voltages/generated currents as a function of time for the various stimulation techniques. Different timescales in (**a**–**c**) versus (**d**–**e**)

DOI 10.1007/978-1-4614-7320-6_603-6

Like the induced electric field **E**, the secondary tissue current **J** (current density in A/m^2) is a vector field, and $\mathbf{J} = \sigma\mathbf{E}$ (σ is the electrical conductivity given in Siemens per meter, S/m). During a stimulation pulse, **E** and **J** have the same time courses that follow the first time derivative of the primary coil current (Fig. 2a, solid line). The stronger the applied magnetic field and the faster the field changes (first time derivative of the magnetic flux density, d**B**/dt), the greater the current induced within the body tissues.

Basic principles of the spatial electric field and current distribution induced by magnetic stimulation are derived from controlled experimental conditions and simplified models (Cohen and Cuffin 1991; Maccabee et al. 1991, 1996; Miranda 2005). The electromagnetically induced tissue current is continuous and closes on itself within the volume conductor. Enclosed are regions where the current flows are zero ("null points"). The spatial distributions of the electromagnetically induced electric fields are different for different coil geometries. Standard coils are circular (round) coils and figure-8 (double circular, butterfly) coils. A figure-8 coil consists of two circular (or D-shaped) coils with opposite current direction placed side by side. In a homogeneous volume conductor, a circular coil held flat to its (planar or spherical) surface induces an annular current flow opposite in direction to the primary coil current and in planes parallel to the air-conductor interface (Fig. 3a). The current density is maximal beneath the windings of the coil and rapidly falls off toward the coil center, while the decay when moving outward from the coil is more gradual. The result is a broad, very non-focal distribution of the induced currents. Some directional sensitivity of the induced current distribution can be achieved by a figure-8 coil (Fig. 3b). The current loops superimpose maximally under the region of the long axis of the junction of the two coil wings. Positioning the junction above a target area produces a maximum current flow through it with currents of lower density returning in circles on both sides.

The suppression of electric field components perpendicular to the volume conductor's surface in contact with the magnetic coil is due to boundary effects. An electric field component perpendicular to a planar infinite boundary is not induced, regardless of the coil type or orientation (the normal component of the current flow at the tissue-air boundary must be zero). Similarly, when paraspinal

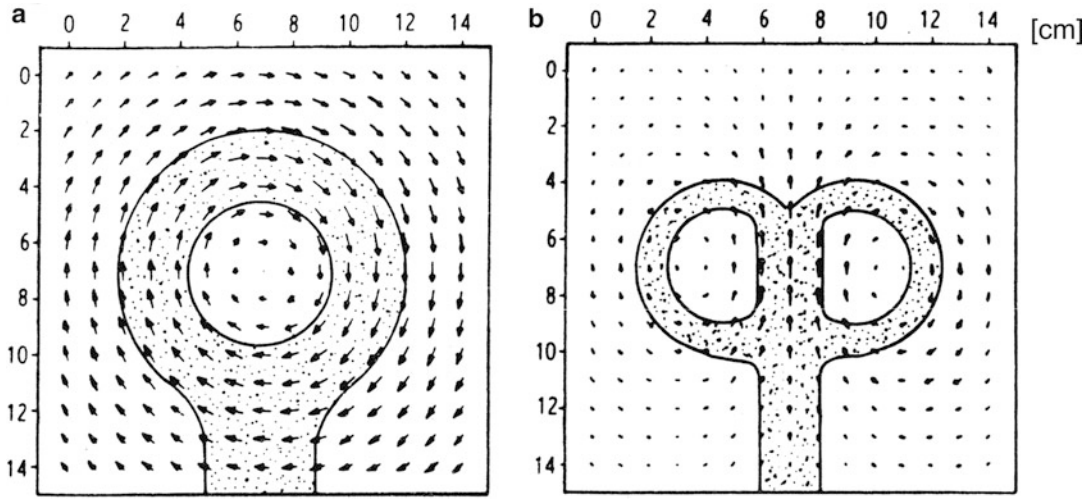

Fig. 3 Electric fields induced by (**a**) a circular and (**b**) a figure-8 magnetic coil oriented flat against the bottom surface of a cylindrical tank filled with isotonic saline. The electric field distributions are represented by current *arrow* diagrams in a plane parallel to the bottom surface; magnitudes and directions are derived from measurements using a coaxial cable probe. The *arrows* are equally spaced, and the relative current densities are indicated by the size of each *arrow* (Reproduced from Maccabee et al. (1991) with permission from Elsevier Scientific Publishers)

DOI 10.1007/978-1-4614-7320-6_603-6

magnetic stimulation is applied, the vectors of the electric field and current density are initially parallel to the boundary of the back as well, and thus the currents induced within the volume conductor are predominantly parallel to the frontal plane. For further information on the biophysics of magnetic stimulation, see Miranda (2005), Epstein (2008), Riehl (2008), and Sommer (2008).

The influence of the spine on the electric field distribution induced by magnetic stimulation was described using human cervical-thoracic and lumbosacral spine segments immersed in a saline-filled container (Maccabee et al. 1991, 1996). The electric fields induced by a circular coil and a large figure-8 coil were measured within the intervertebral foramina, the vertebral canal, and the sacral canal. The direction of the electric field across the intervertebral foramina and within the vertebral canal is similar to that expected in a homogeneous volume conductor. Thus, induced currents enter and exit the spine from its sides. Due to "current-tunneling" effects, the maximum electric field intensities produced in and near an intervertebral foramen are more than two times larger than within the vertebral canal. More importantly, the first-order spatial difference of the electric field across the intervertebral foramen is more than 10 times larger than along the vertebral canal. Accordingly, paraspinal magnetic stimulation preferentially excites fibers within the spinal roots/nerves at the intervertebral foramina (Ugawa et al. 1989). Large-intensity electric field components are induced in several neighboring intervertebral foramina simultaneously. Depending on the coil geometry and orientation with respect to the spine, current flow through the left and right foramina of the same intervertebral level can have the same or opposite directions. Moreover, the direction of current flow through the intervertebral foramina along a given side of the spine can change, with null points in between (e.g., circular coil positioned with its center directly over the spine). While the mediolateral orientation of the intervertebral foramina is ideally channeling the induced electric field, locally concentrating the induced current, such "hot spots" for stimulation are not produced at the anterior sacral foramina with their anteroposterior orientation. Stimulation of neural structures within the vertebral canal requires anatomical conditions that considerably influence the first-order spatial difference of the electric field tangential to the fiber paths. Such inhomogeneity arises at the interface between nerve rootlets and the spinal cord, where the electrical conductivity of the volume conductor as well as the spatial orientation of the fibers with respect to the generated electric field changes abruptly.

Paraspinal Transcutaneous Electrical Stimulation

In paraspinal transcutaneous electrical stimulation, a minimum of two electrodes are placed over the body surface with a configuration to produce tissue currents that partially pass the neural target structures. During a stimulation pulse, a potential difference between the electrodes is built up that causes ionic tissue currents to flow from the anode to the cathode. The current flows according to the electrical conductivities of the tissues and spreads due to the repulsive forces exerted between like charges. The basic principles of the spatial electric field and current distribution generated by paraspinal transcutaneous electrical stimulation are derived from computer models (Ladenbauer et al. 2010; Szava et al. 2011). All currents generated within the volume conductor need to pass the electrode-skin interfaces and flow through several centimeters of low-conductivity tissues to reach the neural targets. High current densities develop directly below the skin electrodes, and less than 10 % of the produced current flows through the volume containing the spinal roots and spinal cord. Close to the stimulating electrodes, the current flow is directed perpendicularly to the electrode-skin interface. Most of the current flows around the spine, while some current enters/exits the spine mainly via the soft tissues with better conductivities in a direction perpendicular to the frontal plane. With symmetrically midline-positioned electrodes, current penetration from the sides into the spine is minimal. The current direction within the spine and vertebral canal also depends on the placement

of the skin electrodes. With cathode and anode placed longitudinally over the back, most of the current flows tangentially to the spinal cord in the vertebral canal, mainly concentrated in the better-conducting cerebrospinal fluid. Moreover, close to the vertebral levels of the paraspinal cathode and anode positions, currents enter/exit the spine in opposite directions. With one electrode over the back and one anteriorly placed (e.g., over the abdomen), the current enters and exits the spine and the vertebral canal in one direction, mainly perpendicularly to the frontal plane.

The stimulation of deep neural structures is made possible by the inhomogeneities of the electrical tissue properties around and within the spine and the bends of the fiber paths of the target neurons. These anatomical influences considerably reduce the thresholds of some neural structures at localized sites and thus create hot spots for external electrical stimulation. Details and biophysical principles are presented in Minassian et al. (2011) and in the entry "▶ Finite Element Models of Transcutaneous Spinal Cord Stimulation." Depolarization sites partially depend on the method of electrical stimulation applied, as well as the vertebral level of stimulation. Hot spots for stimulation predicted by computer modeling are at the interface of the posterior rootlets and the spinal cord (selective stimulation of sensory fibers) and at the distal segments of the posterior and anterior roots close to the intervertebral foramina (Ladenbauer et al. 2010; Danner et al. 2011). In high-voltage stimulation, the most proximal segments of the anterior rootlets at their exits from the spinal cord can be locally targeted as well (de Noordhout et al. 1988).

Two stimulation methods, referred to as "high-voltage (paraspinal) electrical stimulation" and "transcutaneous spinal cord stimulation," are described. They target different neural structures and differ in the time parameters of stimulation (pulse shape and duration) as well as the spatial arrangement of the stimulating electrodes (size and placement).

High-voltage electrical stimulation was primarily designed for supramaximal stimulation of the motor roots as close to their exits from the spinal cord as possible. It uses stimulators as employed in transcranial electrical stimulation of the motor cortex, where high-intensity pulses are applied to penetrate the cranium. Two stimulators are commonly used, the Digitimer D180 and D185 (Digitimer Ltd., Hertfordshire, England, UK). The D180 produces a spike-like pulse with a very fast rise time of 5 μs and a decay constant of either 50 μs or 100 μs and has a maximal output of 750 V (Fig. 2b). The D185 produces a rectangular-like pulse of 50-μs width and has a maximal output of 1,000 V (Fig. 2c). Stimuli are delivered through electrodes with active areas of the cathode smaller than 1 cm^2. With a midline-positioned cathode over the target vertebral level, the anode can be positioned 2–3 vertebral segments rostrally ("conventional longitudinal median montage," Rossini et al. 1994; Troni et al. 1996). More distant anodes, e.g., over the abdomen ("dorsoventral montage," Troni et al. 1996) in the stimulation of lumbosacral roots, produce responses at lower intensities.

Transcutaneous spinal cord stimulation was designed to noninvasively stimulate similar sensory structures as with epidural implants over the lumbar spinal cord (Minassian et al. 2007; Ladenbauer et al. 2010). It uses equipment similar to that in functional electrical stimulation (FES) of paralyzed muscles or in therapeutic transcutaneous electrical nerve stimulation (TENS). By using skin electrodes with large surface areas and applying longer pulse widths (Fig. 2d, e), the thresholds of the targeted neural structures are considerably reduced. This allows using conventional stimulators for continuous stimulation at a fixed frequency for a longer period of time. Stimulators that produce maximum stimulus intensities of 60–100 V (voltage-controlled stimulators) or 120–200 mA (current-controlled stimulators) are appropriate. The large electrodes and moderate stimulation intensities further reduce discomfort (Roy et al. 2012). When stimulation is applied in a continuous mode for neuromodulation applications, the output must be charge balanced to reduce the likelihood of skin damage or irritation. The electrode setups utilize paraspinally placed stimulating electrodes

DOI 10.1007/978-1-4614-7320-6_603-6

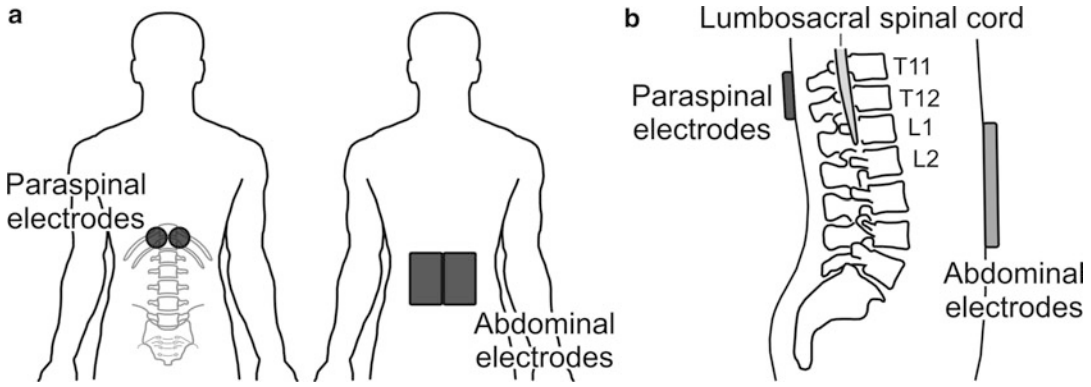

Fig. 4 Transcutaneous spinal cord stimulation. (**a**) Drawings of the stimulation and reference electrodes over the back and abdomen, respectively, and (**b**) of their positions with respect to the spine and spinal cord

and anteriorly placed reference electrodes. The method described in Minassian et al. (2007) uses a pair of round electrodes (diameter 5 cm) over the paraspinal skin with a pair of rectangular reference electrodes (8 × 13 cm each) covering the lower abdomen (Fig. 4). The exact electrode dimensions are not essential, yet relatively large reference electrodes ensure a stronger stimulating effect over the spine. Symmetrical, biphasic rectangular pulses (1 ms width per phase) delivered by a constant-voltage stimulator require low stimulus intensities. The paraspinal electrodes act as cathode when the polarity of the biphasic stimulus pulse is changed at the edge between its first and second phase (Fig. 2e), and neural elements are stimulated at this abrupt change of polarity. Alternative stimulation setups use reference electrodes placed over the iliac crests (Dy et al. 2010; Roy et al. 2012). For further details, see Minassian et al. (2011).

Stimulated Neural Structures, Site of Excitation, and Evoked Muscle Responses

Paraspinal Magnetic Stimulation

Magnetic stimulation over the cervical and lumbar spinal cord normally excites motor fibers within the anterior roots/spinal nerves at the intervertebral foramina (Ugawa et al. 1989). The evoked responses, recorded with surface electrodes as compound muscle action potentials (CMAPs) from the respective muscles, are hence M-waves. The onset latencies of these M-waves are shorter than the total peripheral motor conduction time by the segment from the anterior horn cells to the intervertebral foramen. These onset latencies remain constant when moving the coil over the spine for some centimeters in rostral or caudal direction to the lowest-threshold site. Only with maximum stimulation, the sites of excitation along the motor fibers may migrate distally beyond the intervertebral foramina. Paraspinal magnetic stimulation does not allow for reliable supramaximal stimulation. Maximum attainable response amplitudes range from 10 % to 90 % of the maximal peripheral nerve M-wave. Large-amplitude responses cannot be obtained simultaneously in multiple muscles of a limb from a single stimulation site. Custom-made, large circular coils can be used to overcome some of these limitations (Matsumoto et al. 2009a). M-waves in response to magnetic stimulation over the cervical-thoracic spine are described in various C5-T1 innervated muscles of the shoulder (deltoid), arm (biceps, brachioradialis, extensor digitorum), and hand (thenar and hypothenar muscle groups). These responses have the lowest thresholds and are largest when the secondary tissue current is directed over the intervertebral foramina of the target motor roots and

flows from the midline toward the side. Such stimulation favors unilateral excitation (Mills et al. 1993). For details on coil placements, see Ugawa et al. (1989), Mills et al. (1993), Rossini et al. (1994), and Sandbrink (2008). Stimulation over the mid-thoracic spine (T7-T9) evokes M-waves in the abdominal and intercostal muscles (Chokroverty et al. 1995). Magnetic stimulation over the lumbosacral spine elicits M-waves in the muscles of the upper and lower leg and the foot (e.g., quadriceps femoris, tibialis anterior, gastrocnemius, extensor digitorum brevis, flexor hallucis brevis, and abductor hallucis). For stimulating lumbar roots exiting the spine through the intervertebral foramina, the induced current can be concentrated through these hot spots of stimulation when oriented from side to side, and motor fibers are activated at the most distal portion of the cauda equina. The situation is different for muscles with motor roots exiting from the anterior sacral foramina. With the coil held over the sacral bone, the sacral roots are stimulated in the most distal portion of the cauda equina, as suggested by the very short onset latencies of the M-waves, but the exact site of stimulation is not completely clear (Maccabee et al. 2011). For details, see Ugawa et al. (1989) and Maccabee et al. (1996).

A second localized activation site of the motor fibers is within the vertebral canal at the interface between the spinal cord and the anterior rootlets. Activation at these proximal sites is reported for magnetic stimulation over the lumbosacral spinal cord and requires large coils and the induced tissue currents to be directed rostrally (Maccabee et al. 1996, 2011; Matsumoto et al. 2009b). Thresholds at these proximal hot spots are higher than those at the intervertebral foramina. M-waves elicited proximally are similar in appearance to those elicited in the distal cauda equina, but the onset latencies are longer by 1.9 ms for the vastus medialis, 2.3 ms for the tibialis anterior, and 3.5 ms for the abductor hallucis (Maccabee et al. 1996). The straight, relatively long intrathecal segments of the lumbosacral motor fibers between their two low-threshold sites are normally not activated by magnetic stimulation.

Apart from the M-wave, a second type of muscle response can be evoked by magnetic stimulation, i.e., a CMAP constituted of two partially superimposed response components, an M-wave and a later response with electrophysiological characteristics similar to the H-reflex (Maccabee et al. 1996). Such composite responses are only evoked in few lower limb muscles and with stimulation over the distal cauda equina. The H-reflex is a monosynaptic reflex usually initiated by the electrical stimulation of Ia afferent fibers from muscle spindles at the posterior knee and recorded from the soleus muscle. A "pure" H-reflex without contamination by a preceding M-wave is normally not obtained by magnetic stimulation.

There is no evidence for the direct electrical stimulation of neural structures within the spinal cord white or gray matter by magnetic coils. Paresthesias (tingling sensations) or motor responses in the lower limbs are not evoked with magnetic stimulation over the cervical-thoracic spine (Ugawa et al. 1989). Thus, stimulation of myelinated, large-diameter, and relatively superficially located fibers within long tracts of the spinal cord white matter does not occur. It is estimated that a sevenfold increase of the maximum output of conventional magnetic stimulators would be required for their excitation (Maccabee et al. 1991). Consequently, the direct electrical stimulation of the spinal cord gray matter interneurons or neural networks, which would require even higher thresholds, is considered impossible.

High-Voltage Electrical Stimulation

The principal neural targets of high-voltage paraspinal electrical stimulation are the motor roots, and the evoked responses are M-waves (Rossini et al. 1994). Midline-positioned electrodes activate muscles bilaterally and symmetrically (i.e., at similar thresholds). High-voltage electrical stimulation over the cervical spine excites motor fibers innervating the upper limb muscles. The site of

DOI 10.1007/978-1-4614-7320-6_603-6

excitation is within the anterior roots/spinal nerves close to the respective intervertebral foramina, estimated 2–4 cm distal to the anterior horn cells (Mills and Murray 1986). The latencies of the M-waves evoked in the upper limb are about 1.2–1.6 ms shorter than the total peripheral motor conduction time (Mills and Murray 1986; Rossini et al. 1994). At moderate stimulus intensities, the response latencies remain unchanged when moving the electrode in vertical or horizontal direction for several centimeters. With the cathode over the T1 vertebra and the anode over the C5 vertebra, all motor roots to the upper limb muscles are recruited (Rossini et al. 1994). A more selective stimulation is achieved by placing the cathode over the vertebra of the corresponding exit level of the target motor root, with a distant anode over the contralateral shoulder (Ugawa et al. 1989). High-voltage electrical stimulation over the cervical enlargement allows for supramaximal stimulation of the cervical motor roots, with maximum upper limb muscle responses at 250–300 V.

For stimulation over the lumbosacral spine, two low-threshold sites for the activation of the motor fibers can be distinguished. Cathodes over T11-L1 vertebral levels, corresponding to the level of the lumbosacral spinal cord, excite the motor fibers within the anterior rootlets at their exits from the spinal cord (de Noordhout et al. 1988; Troni et al. 2011). Cathodes over L3-S1 vertebral levels activate the anterior roots/spinal nerves close to the respective intervertebral foramina (de Noordhout et al. 1988). At very strong stimulus intensities, the motor roots may be activated at some site in between these low-threshold sites (de Noordhout et al. 1988). M-waves in the lower limbs have similar CMAP shapes when elicited from both low-threshold sites, but with the more distal stimulation, the onset latencies decrease by 1.4 ± 0.6 ms for the quadriceps, 2.4 ± 1.2 ms for the tibialis anterior, and 3.0 ± 1.0 ms for the extensor digitorum brevis (de Noordhout et al. 1988). With the cathode placed midline over the spine and the anode over the contralateral iliac crest, threshold intensities for CMAPs elicited in the lower limb muscles range from 225 to 450 V, and maximum responses are obtained at 450–600 V (de Noordhout et al. 1988; Ugawa et al. 1989). A single stimulus pulse applied from a fixed stimulation site can generate simultaneous supramaximal stimulation of the L3-S1 motor roots when using a dorsoventral montage (Troni et al. 2011).

Both a direct M-wave and a later response similar to the H-reflex can be evoked in the soleus by high-voltage electrical stimulation over the T11-S1 vertebral levels (de Noordhout et al. 1988; Troni et al. 1996), hinting on the activation of large-diameter proprioceptive fibers in addition to motoneuron axons. The difference between the M-wave and reflex-response latencies is 1.2 ± 0.2 ms for stimulation over the lumbosacral spinal cord and 5.4 ± 0.9 ms for stimulation of the distal cauda equina (Troni et al. 1996). With the elicitation of maximal M-waves, the reflex component is canceled.

Maximal high-voltage electrical stimulation over the cervical-thoracic spine evokes low-amplitude responses in some lower limb muscles innervated by distant lumbar and upper sacral spinal cord segments (Mills and Murray 1986; Taylor and Gandevia 2004). In the relaxed muscle, they normally attain amplitudes <10 % of the maximum M-wave evoked by electrical peripheral nerve stimulation. The thresholds of these responses are 300–750 V and are always higher than those of the M-waves evoked by the stimulation of the nearby spinal nerves. The distant responses result from the electrical stimulation of descending corticospinal tracts of the spinal cord white matter and the transsynaptic activation of lumbosacral motoneurons innervating the lower limb muscles. They are thus motor-evoked potentials and due to the stimulation of similar populations of corticospinal axons as activated by transcranial stimulation of the motor cortex (Martin et al. 2008). The exact site of stimulation along the corticospinal axons below the stimulating paraspinal electrodes is not defined.

Encyclopedia of Computational Neuroscience
DOI 10.1007/978-1-4614-7320-6_603-6

Transcutaneous Spinal Cord Stimulation

The targeted neural structures of transcutaneous spinal cord stimulation are sensory fibers projecting into the spinal cord. For stimulation over the T11-T12 spinous processes, overlying the lumbar spinal cord, the low-threshold sites are at the entries of the posterior rootlets into the spinal cord (Minassian et al. 2011). The evoked responses result from the electrical stimulation of Ia muscle spindle afferents and the subsequent monosynaptic activation of motor fibers innervating the lower limb muscles. According to their initiation and recording sites, they were termed posterior root-muscle (PRM) reflexes (Minassian et al. 2007). Alternative terminologies were suggested (Dy et al. 2010; Roy et al. 2012). A single pulse can consistently activate L2-S2 posterior root fibers bilaterally and thus evoke PRM reflexes in essentially all lower limb muscles simultaneously. Transcutaneous spinal cord stimulation thus activates similar populations of sensory fibers as stimulation through epidural implants over the lumbar spinal cord (Fig. 5).

PRM reflexes have some electrophysiological similarities with the H-reflex (Minassian et al. 2011). They are enhanced by background voluntary activation of the target muscle and suppressed by contraction of the antagonist muscles or vibration applied on the tendons of the lower limbs. They are further characterized by excitability changes lasting up to 10 s following a prior stimulus. The simultaneous stimulation of multiple posterior roots results in transsynaptic effects other than (homonymous) monosynaptic excitation that may influence the PRM reflex of the target muscle, particularly when repetitively elicited in close succession (Minassian et al. 2011; Roy et al. 2012). Onset latencies of PRM reflexes to single pulses applied at incremental intensities to the lumbar spinal cord stay invariant and amount to 10.3 $\pm$ 1.1 ms for the quadriceps, 11.2 $\pm$ 0.4 ms for the hamstrings, 19.1 $\pm$ 0.9 ms for the tibialis anterior, and 19.7 $\pm$ 1.1 ms for the triceps surae (Minassian et al. 2007). Thresholds for eliciting PRM reflexes depend on the pulses applied (mono- or biphasic and their polarities), the individual physique, and the body position (e.g., supine or standing) and range from 20 to 40 V or 40 to 120 mA. The preferential activation of sensory roots minimizes an occlusion of the PRM reflex caused by antidromic volleys in the motor roots. Maximum PRM reflexes may attain amplitudes of up to 76 % of the corresponding maximum M-wave (Kitano and Koceja 2009) and depend on the excitability of the monosynaptic reflex in the target muscle (Roy et al. 2012).

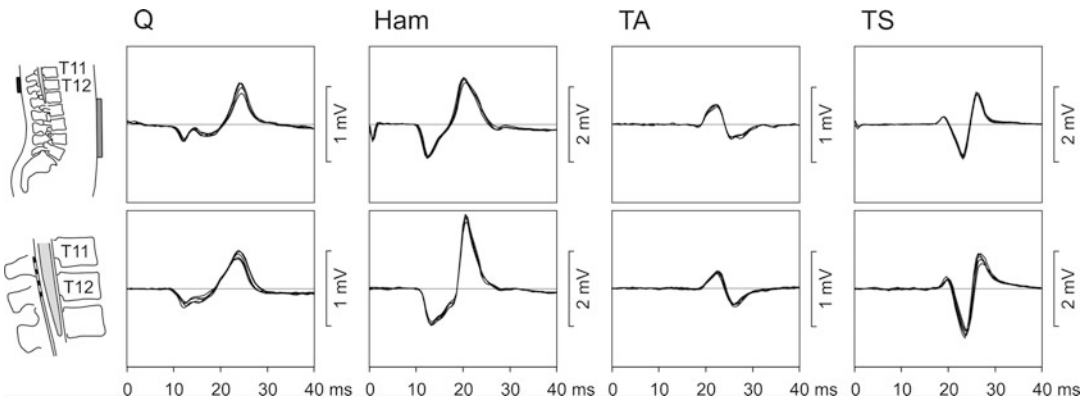

Fig. 5 Posterior root-muscle (*PRM*) reflexes evoked by transcutaneous and epidural spinal cord stimulation in the quadriceps (*Q*), hamstrings (*Ham*), tibialis anterior (*TA*), and triceps surae (*TS*) in a single incomplete spinal cord-injured individual. The similarities of PRM reflexes elicited by either technique imply that transcutaneous stimulation depolarizes (a subset of) the same neural structures as activated by implanted epidural electrodes (For details, see Ladenbauer et al. 2010; Minassian et al. 2011)

DOI 10.1007/978-1-4614-7320-6_603-6

Stimulation over the cauda equina (e.g., at L4-L5 vertebral levels) at incremental intensities results in a characteristic sequence of PRM reflex and M-wave elicitation, similar to the recruitment of sensory and motor fibers by stimulation of a mixed peripheral nerve (Minassian et al. 2007, 2011). Activation sites are at the intervertebral foramina, where posterior and anterior roots approach each other to form the spinal nerve. M-waves only are elicited in muscles innervated by the upper lumbar roots, e.g., quadriceps, that exit the spine rostral to such stimulation site. At threshold intensity, PRM reflex latencies are 13.3 ± 1.0 ms for the hamstrings, 21.1 ± 1.0 ms for the tibialis anterior, and 21.3 ± 1.1 ms for the triceps surae (Minassian et al. 2007). For stimulation sites between the T11-T12 vertebrae and the distal cauda equina, M-wave and reflex contributions to the evoked composite CMAPs vary, depending on the position of the cathode along the lumbar spine (Roy et al. 2012).

Continuous transcutaneous stimulation (e.g., 30 Hz) over the T11-T12 vertebral levels produces paresthesias in the lower limb dermatomes (Hofstoetter et al. 2013b) that are normally associated with the stimulation of ascending sensory fiber branches within the posterior columns of the spinal cord white matter. The direct stimulation of the posterior columns is further suggested by the distribution of the paresthesias when graded stimulation is applied; with electrode placements evoking muscle responses in L2-L4 myotomes at threshold intensity, paresthesias are often produced in the L5-S2 dermatomes first. Yet computer simulations suggest that posterior column fibers have considerably higher thresholds than posterior root fibers; see Danner et al. (2011) and the entry "► Finite Element Models of Transcutaneous Spinal Cord Stimulation." Alternatively, the paresthesias can be explained by the stimulation of fibers from cutaneous receptors within the posterior roots as well.

Figure 6 summarizes the stimulated neural structures and their excitation sites for paraspinal magnetic and electrical stimulation.

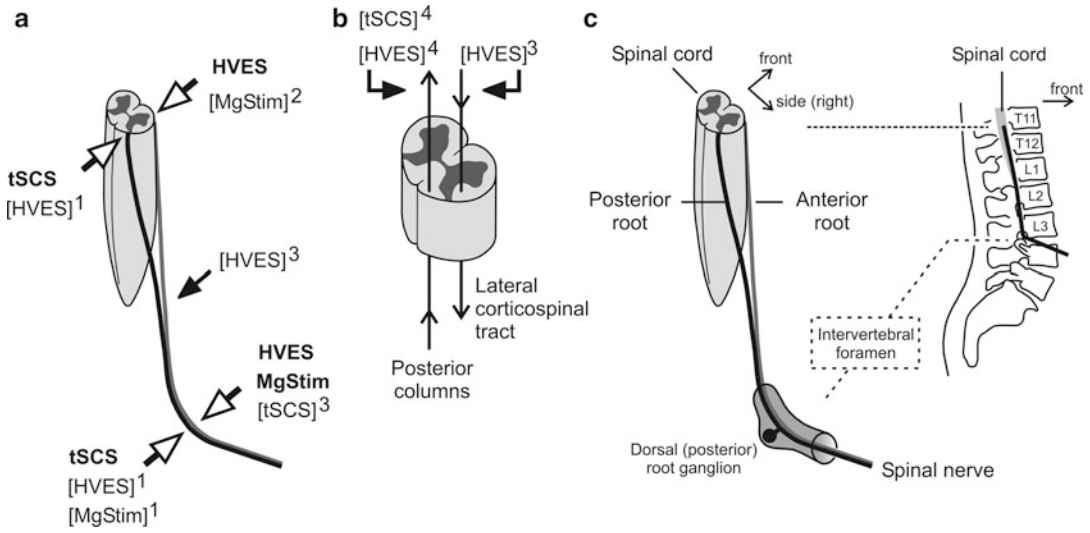

Fig. 6 Summary of neural structures directly stimulated by paraspinal magnetic (*MgStim*), high-voltage paraspinal electrical (*HVES*), and transcutaneous spinal cord stimulation (*tSCS*), respectively. Stimulation of (**a**) spinal root fibers and (**b**) long-tract fibers of the spinal cord white matter. Methods given in brackets indicate that stimulation is effective under specific conditions: (1) reported in few muscles only, (2) only effective with specific magnetic coils and tissue current directions, (3) only with maximal stimulation intensities, and (4) not unequivocally demonstrated. *Open arrowheads* mark low-threshold sites of stimulation. (**c**) Drawing of the relevant anatomical structures; separation of the roots into several rootlets before entering the spinal cord is not illustrated

Encyclopedia of Computational Neuroscience
DOI 10.1007/978-1-4614-7320-6_603-6

Applications

Lower Motoneuron Stimulation

Functional Assessment of the Cauda Equina and the Motor Root Conduction Time

One of the main clinical applications of paraspinal magnetic or high-voltage electrical stimulation is the neurodiagnostic assessment of the functional integrity of deeply located peripheral motor fibers. Within the cauda equina, the most proximal segments of the motor fibers can be affected by focal lesions caused by mechanical impacts to the spinal roots or root compressions. They are also involved in demyelinating peripheral neuropathies, with a degeneration of the myelin sheaths that slows down or completely blocks the conduction of action potentials. A method to assess the cauda equina is by the evaluation of the motor root conduction time (MRCT). The MRCT is calculated as the difference between the total peripheral motor conduction time (PMCT) and the latency of the CMAP evoked by conventional paraspinal magnetic stimulation. The total PMCT is estimated by the F-wave method; for details, see Rossini et al. (1994) and Sandbrink (2008). The MRCT is the conduction time between the anterior horn cells and the actual site of activation of the motor fibers by paraspinal stimulation at the intervertebral foramen. Given a focal spinal root lesion, this neural excitation site would be distal to the affected segment of the motor fiber, and the latency of the CMAP would be normal, while the total PMCT would be delayed. The applicability of this method relies on the presence of F-waves and is therefore limited to a few distal muscles.

Alternatively, the lumbosacral MRCT can be estimated by paraspinal stimulation of the motor fibers at their two low-threshold sites, i.e., within the proximal and distal cauda equina, respectively. Large circular (Matsumoto et al. 2009b) and figure-8 (Maccabee et al. 1996) magnetic coils (both not commonly used in clinical practice), as well as high-voltage electrical stimulation (de Noordhout et al. 1988), can activate the most proximal segments of the motor fibers at their origin from the spinal cord and their more distal portions at the cauda equina. The difference between the proximal and distal response latencies is the MRCT (or cauda equina conduction time, CECT; Maccabee et al. 2011). The CECT can be calculated for several roots simultaneously when recording CMAPs from multiple lower limb muscles. The total PMCT can be broken up into separate segments, including the cauda equina, upper leg, and lower leg conduction times (Maccabee et al. 2011). Axonal and (subtypes of) demyelinating neuropathies can be differentiated depending on the contributions of proximal or distal axon segments to the slowing of conduction. Axonal neuropathy involves degeneration of the entire axon rather than of the myelin sheath around the axon only, with the degeneration usually advancing from the axon's most distal portions toward the cell body.

The detection of cauda equina lesions and conduction blocks based on the measurement of the CMAP amplitude or area requires a technique providing for supramaximal stimulation, a criterion not fulfilled by conventional magnetic stimulation. High-voltage paraspinal electrical stimulation ensures supramaximal activation and can activate motor fibers within the anterior rootlets at their origin from the spinal cord, allowing for the exploration of the complete proximal nerve tract. The discomfort induced by high-voltage electrical stimulation is described as acceptable to excessive.

The cervical spinal nerves in the vertebral canal are short, and their conduction times have limited relevance for clinical diagnostics. The cervical MRCT can be calculated based on F-wave latencies and the response to paraspinal stimulation over the respective intervertebral foramina. Magnetic stimulation over the cervical and thoracic spine may be useful in the study of other deeply located nerves, such as the phrenic nerve and thoracic spinal nerves for the evaluation of nerve conduction velocity of the respiratory muscles. For details, see Rossini et al. (1994), Di Lazzaro and Oliviero (2005), and Sandbrink (2008).

DOI 10.1007/978-1-4614-7320-6_603-6

Central Motor Conduction Time

Paraspinal stimulation combined with transcranial stimulation is used to calculate the conduction time in the fastest propagating central motor axons (i.e., axons of the upper motoneurons of the corticospinal tracts). Motor-evoked potentials (MEPs) elicited by transcranial stimulation of the motor cortex and electromyographically recorded from the target muscles provide for a noninvasive assessment of neurological disorders with upper motoneuron involvement. In clinical routine, the most important MEP parameter is the central motor conduction time (CMCT). The CMCT is the central component of the total MEP latency, i.e., the time from the stimulation of the cortex to the transsynaptic activation of the spinal motoneurons. The CMCT is obtained by subtracting the PMCT from the total MEP latency. The PMCT is estimated either by F-wave measurements or by paraspinal stimulation of the motor roots. For routine applications of motor root stimulation, many laboratories use conventional paraspinal magnetic stimulation. Since this method activates the motor roots in the region of the intervertebral foramen, the $CMCT_{mgn}$ calculated includes the conduction time along the anterior root and is estimated as too long (by 0.5–1.4 ms for cervical root stimulation and 3.0–4.1 ms for lumbosacral root stimulation; Sandbrink 2008). MEPs and the measurement of the CMCT can document corticospinal-tract involvement in patients with clinically evident upper motoneuron lesions. Further, the method may detect subclinical lesions, i.e., changes of the conduction properties of the corticospinal tract prior to clear clinical signs. Prolongation of the CMCT occurs with demyelination of the corticospinal fibers that contribute to the MEP, as in multiple sclerosis or segmental demyelination due to mechanical compression of the spinal cord (spondylosis or disk herniation). When recording from multiple muscles associated with different spinal cord segmental levels, the method may help identify the (rostrocaudal) location of a spinal cord lesion as well as assess mixed conus-cauda injuries. For further information, see Di Lazzaro and Oliviero (2005) and Sandbrink (2008).

Intraoperative Neuromonitoring

Nerve root damage is a potential neurological complication in lumbosacral spine surgery. High-voltage electrical stimulation of the proximal cauda equina can be applied to survey nerve root function during such surgery and to prevent potential damage to the nervous system. The principle is to provide for early detection of a nerve injury in an acute yet reversible state, hence allowing for immediate corrective procedures during surgery. During brief suspensions of the surgical procedure, single pulses are applied to produce supramaximal stimulation of the lumbosacral motor roots above the level of the surgical procedure. CMAPs are recorded from several muscles bilaterally innervated by L2-S2 spinal roots. Potential mechanical stress on the roots is immediately detected as a transient reduction of the CMAP amplitude in the respective muscles, caused by a conduction failure in the manipulated root. The technique is described in anesthetized patients undergoing lumbosacral surgery in degenerative spinal diseases (Troni et al. 2013).

Functional Magnetic Stimulation (FMS)

FMS produces patterned muscle contractions for useful bodily functions in people with upper motoneuron dysfunction. To this end, FMS applies timed, short sequences of repetitive magnetic stimulation (e.g., bursts of 25-Hz stimulation for 2 s) to the respective lower motoneurons. When the spinal cord is damaged, muscles below the level of the injury become (partially) paralyzed. Such paralysis does not only impede the ability to move but normally also affect the respiratory muscles, the gastrointestinal tract, and the bladder. Major muscles of inspiration include the diaphragm (primarily innervated by the phrenic nerve formed from the cervical nerves C3-C5), the parasternal muscles, and the external intercostal muscles (T1-T6 spinal nerves). Major muscles of expiration

DOI 10.1007/978-1-4614-7320-6_603-6

include the abdominal muscles (T7-L1 spinal nerves) and the internal intercostal muscles. Thus, with levels of injury from T12 to more rostral vertebrae, there is a progressive loss of respiratory motor function, with impairment of expiration and cough, further impairment of inspiratory and expiratory function, and weakened respiration to the point at which ventilation cannot be self-sustained. FMS can be applied over the appropriate vertebral levels and to the respective motor roots to generate inspired and expired pressures. FMS of the cervical and upper thoracic nerves produces inspired volume and pressure and may be useful for enhancing inspiratory function and muscle conditioning. Similarly, FMS of the lower thoracic nerves produces expired volume and pressure and can be effective for simulating or restoring cough. An important advantage of FMS is that expiratory muscle activation can be achieved noninvasively. For limitations of the technique, see DiMarco (2005). Additional clinical applications of FMS include the stimulation of the sacral nerves for enhancing micturition and defecation function in selected spinal cord-injured persons with neurogenic bladder and bowel. For details on FMS as a therapeutic tool, see Lin and Hsiao (2005).

Corticospinal-Tract Stimulation

Evaluation of Corticospinal-Tract Function

The clinical value of high-voltage paraspinal electrical stimulation of corticospinal axons as a neurodiagnostic method is unclear. In principle, transcranial magnetic stimulation over the motor cortex together with high-voltage paraspinal stimulation at different vertebral levels may help localize alterations of the conduction properties along the fastest descending corticospinal axons and define the level of a spinal cord lesion. However, the technique does not allow for supramaximal activation, and the exact site of stimulation of the corticospinal tract below the paraspinal electrodes is not clear. Furthermore, with low-thoracic and more caudal stimulation sites, antidromic volleys within the posterior columns may add to the evoked response (Zidar 2001).

Human Motor Control Studies

High-voltage paraspinal stimulation of corticospinal axons may provide a measure of motoneuronal excitability for studying motor control of the lower limbs. The evoked responses are modulated in amplitude by volitional motor tasks (Martin et al. 2008). These modifications provide information on the synaptic inputs onto the target motoneuron pools at the level of the spinal cord. The role of the corticospinal pathway in human motor control is normally investigated by transcranial magnetic stimulation over the motor cortex to evoke MEPs. Modulations of transcranially evoked MEPs during motor tasks can result from excitability changes within the motor cortex as well as at spinal cord segmental levels. In combination with transcranial magnetic stimulation, paraspinal stimulation may help identify changes of excitability at the motor cortex by providing a control for changes occurring at the lumbosacral segmental level (Martin et al. 2008).

Posterior Root Stimulation

Human Motor Control Studies

The H-reflex is a major noninvasive tool in human motor control studies. Due to the monosynaptic connections of Ia muscle spindle afferents to motoneurons, the H-reflex can be used to investigate excitability changes of the motoneuron pool supplied by the stimulated nerve. Transcutaneous posterior root stimulation extends H-reflex studies of a single muscle to the simultaneous assessment of monosynaptic reflexes at multiple lumbosacral segmental levels. This is relevant because motor control is organized multisegmentally, involving many muscles with state- and dynamic phase-dependent changes of their functional roles. Furthermore, posterior root stimulation can elicit monosynaptic reflexes in muscles that cannot be investigated by conventional peripheral nerve

stimulation. PRM reflex modifications by motor tasks and passive movements were described in supine and standing positions and during treadmill stepping in subjects with intact nervous system as well as spinal cord injury (Minassian et al. 2007; Hofstoetter et al. 2008; Dy et al. 2010). For further details, see Minassian et al. (2011) and Roy et al. (2012).

Neuromodulation Applications

Neuromodulation therapies aim at improving functions in people with neurological disorders by continuous electrical or neuropharmacological stimulation of specific neural networks of the central nervous system. Electrical stimulation methods in movement disorders, such as deep brain stimulation or epidural spinal cord stimulation, utilize electrodes implanted close to the input structures to the target neural networks. For the enhancement of motor control of the lower limbs by epidural spinal cord stimulation, local locomotor networks within the lumbar spinal cord are the natural targets. These networks are involved in the control of muscle tone, can execute stereotyped lower limb movements, and may remain functional below a severe damage to the spinal cord. Epidural lumbar spinal cord stimulation can control spinal spasticity (Dimitrijevic et al. 1986; Pinter et al. 2000), generate sustained extension (Jilge et al. 2004) and automatic flexion-extension movements of paralyzed lower limbs (Dimitrijevic et al. 1998; Minassian et al. 2004), facilitate task-specific training in clinically motor complete Harkema et al. 2011 and incomplete (Herman et al. 2002) spinal cord-injured individuals, and enhance endurance in people with residual walking capabilities (Huang et al. 2006). In many applications, the effects temporarily persist after the stimulation has been interrupted. For a review, see Minassian et al. (2012). Epidural lumbar spinal cord stimulation does not activate the locomotor networks directly but transsynaptically through large-diameter sensory fibers, predominantly within the posterior roots.

The consistent stimulation of these input structures also by transcutaneous spinal cord stimulation allows for its application as a neuromodulation method. When continuously applied, e.g., at a frequency of 30 Hz or 50 Hz, a “tonic drive” can be provided to the spinal cord below a lesion. Therapeutic applications of such tonic transcutaneous stimulation to alleviate spinal spasticity and enhance neural control of locomotion after spinal cord injury are being investigated (Minassian et al. 2011, 2012; Hofstoetter et al. 2013a, b). For the temporary modification of lower limb spasticity, 50-Hz stimulation is applied for 30 min in a supine position. The intensity is below the threshold for PRM reflexes but produces paresthesias in the lower limbs in individuals with remaining sensory functions. Various manifestations of lower limb spasticity, such as clonus, spasms, and increased muscle tone, are modified after stimulation without loss of residual voluntary control (Hofstoetter et al. 2013b). During assisted, body-weight-supported treadmill stepping, continuous stimulation (e.g., 30 Hz) above the threshold for PRM reflexes has several effects in motor complete spinal cord-injured individuals, including suppression of clonus-like activities, augmentation of EMG activities of the paralyzed lower limb muscles generated by passive treadmill stepping, and generation of stereotyped, rhythmic EMG patterns not linked to the externally imposed gait cycle (Minassian et al. 2012). In motor incomplete spinal cord-injured persons performing active treadmill stepping, tonic transcutaneous stimulation at a sub-motor threshold level, producing paresthesias in the lower limb dermatomes, can immediately modify the voluntarily generated lower limb activities in a gait-phase appropriate way (Fig. 7). Augmented yet consciously controlled muscle activity may also lead to changes of the step kinematics, mainly to increase maximum hip flexion angles and changes in stride length (Hofstoetter et al. 2013a). Further, 15-Hz stimulation can generate bilateral lower limb extension appropriate to produce a standing-up movement in spinal cord-injured people. As an assessment method, tonic transcutaneous posterior

DOI 10.1007/978-1-4614-7320-6_603-6

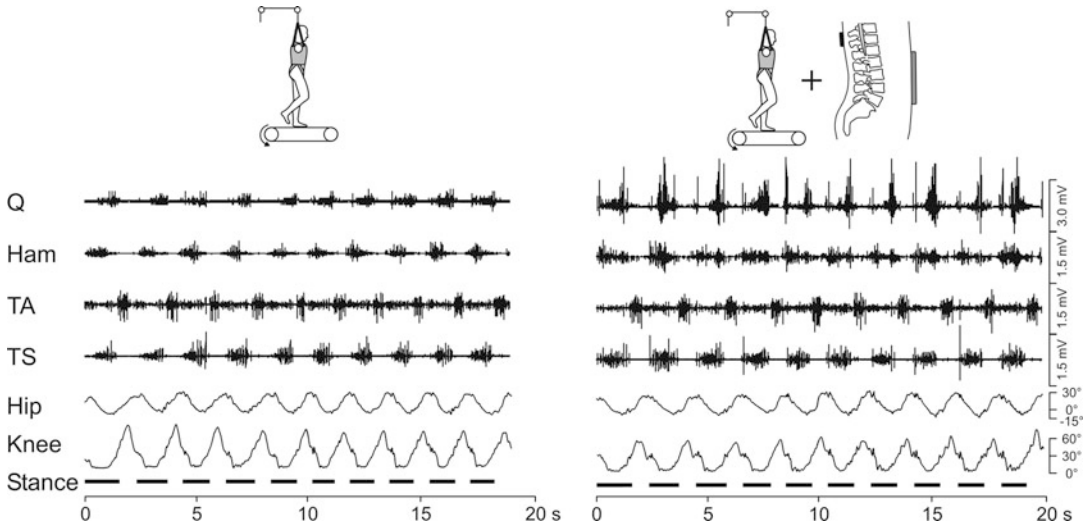

Fig. 7 Volitional treadmill stepping at 2 km/h of an incomplete spinal cord-injured person without and during the application of 30-Hz transcutaneous lumbar spinal cord stimulation. Electromyographic activities of the right quadriceps (*Q*), hamstrings (*Ham*), tibialis anterior (*TA*), and triceps surae (*TS*) along with goniometer recordings of hip and knee angles and stance-phase markers. No manual assistance and body weight support provided. Stimulation was applied over the T11-T12 spinous processes at 27 V, an intensity generating paresthesias in the lower limb dermatomes without eliciting PRM reflexes

root stimulation may provide information on the altered physiology of spinal cord neural networks and can be complementary to the assessment via fast- and slow-conducting descending pathways.

Further Applications

Applications of paraspinal stimulation were described with evident neuromodulative effects but with the directly activated neural structures and the resulting physiological effects remaining speculative. Repetitive magnetic stimulation over the thoracic and lumbar spine reduces motoneuron excitability and spastic muscle tone in patients with spinal lesions (Nielsen and Sinkjaer 1997; Krause et al. 2004). Anodal direct current stimulation over the thoracic spine at 2–2.5 mA for 15–20 min modulates the excitability of central pain pathways in individuals with intact nervous system (Cogiamanian et al. 2011) and modifies spinal reflex activities in motor complete spinal cord-injured people (Hubli et al. 2013).

Acknowledgments

We wish to acknowledge the support of the Vienna Science and Technology Fund (WWTF), Proj.Nr. LS11–057, and the Wings for Life Spinal Cord Research Foundation (WfL), Proj.Nr. WFL-AT-007/11. Special thanks are due to Frank Rattay for his insightful comments and to Martin Schmoll for his support in preparing the illustrations.

DOI 10.1007/978-1-4614-7320-6_603-6

Cross-References

- ▶ Finite Element Modeling for Extracellular Stimulation
- ▶ Finite Element Models of Transcutaneous Spinal Cord Stimulation
- ▶ General Overview of Spinal Anatomy and Physiology

References

Chokroverty S, Deutsch A, Guha C, Gonzalez A, Kwan P, Burger R, Goldberg J (1995) Thoracic spinal nerve and root conduction: a magnetic stimulation study. Muscle Nerve 18:987–991

Cogiamanian F, Vergari M, Schiaffi E, Marceglia S, Ardolino G, Barbieri S, Priori A (2011) Transcutaneous spinal cord direct current stimulation inhibits the lower limb nociceptive flexion reflex in human beings. Pain 152:370–375

Cohen D, Cuffin BN (1991) Developing a more focal magnetic stimulator, part I: some basic principles. J Clin Neurophysiol 8:102–111

Danner SM, Hofstoetter US, Ladenbauer J, Rattay F, Minassian M (2011) Can the human lumbar posterior columns be stimulated by transcutaneous spinal cord stimulation? A modeling study. Artif Organs 35:257–262

de Noordhout AM, Rothwell JC, Thompson PD, Day BL, Marsden CD (1988) Percutaneous electrical stimulation of lumbosacral roots in man. J Neurol Neurosurg Psychiatry 51:174–181

Di Lazzaro V, Oliviero A (2005) Evaluation of myelopathy, radiculopathy, and thoracic nerve. In: Hallett M, Chokroverty S (eds) Magnetic stimulation in clinical neurophysiology, 2nd edn. Elsevier, Philadelphia, pp 105–127

DiMarco AF (2005) Restoration of respiratory muscle function following spinal cord injury. Review of electrical and magnetic stimulation techniques. Respir Physiol Neurobiol 147:273–287

Dimitrijevic MM, Dimitrijevic MR, Illis LS, Nakajima K, Sharkey PC, Sherwood AM (1986) Spinal cord stimulation for the control of spasticity in patients with chronic spinal cord injury: I. Clinical observations. CNS Trauma 3:129–144

Dimitrijevic MR, Gerasimenko Y, Pinter MM (1998) Evidence for a spinal central pattern generator in humans. Ann N Y Acad Sci 860:360–376

Dy CJ, Gerasimenko YP, Edgerton VR, Dyhre-Poulsen P, Courtine G, Harkema SJ (2010) Phase-dependent modulation of percutaneously elicited multisegmental muscle responses after spinal cord injury. J Neurophysiol 103:2808–2820

Epstein CM (2008) TMS stimulation coils. In: Wassermann EM, Epstein CM, Ziemann U, Walsh V, Paus T, Lisanby SH (eds) The Oxford handbook of transcranial stimulation. Oxford University Press, New York, pp 25–32

Harkema S, Gerasimenko Y, Hodes J, Burdick J, Angeli C, Chen Y, Ferreira C, Willhite A, Rejc E, Grossman RG, Edgerton VR (2011) Effect of epidural stimulation of the lumbosacral spinal cord on voluntary movement, standing, and assisted stepping after motor complete paraplegia: a case study. Lancet 377:1938–1947

Herman R, He J, D'Luzansky S, Willis W, Dilli S (2002) Spinal cord stimulation facilitates functional walking in a chronic, incomplete spinal cord injured. Spinal Cord 40:65–68

Hofstoetter US, Minassian K, Hofer C, Mayr W, Rattay F, Dimitrijevic MR (2008) Modification of reflex responses to lumbar posterior root stimulation by motor tasks in healthy subjects. Artif Organs 2:644–648

Hofstoetter US, Hofer C, Kern H, Danner SM, Mayr W, Dimitrijevic MR, Minassian K (2013a) Effects of transcutaneous spinal cord stimulation on voluntary locomotor activity in an incomplete spinal cord injured individual. Biomed Tech (Berl). doi:10.1515/bmt-2013-4014

Hofstoetter US, McKay WB, Tansey KE, Mayr W, Kern H, Minassian K (2013b) Modification of spasticity by transcutaneous spinal cord stimulation in individuals with incomplete spinal cord injury. J Spinal Cord Med 37(2):202–211. doi:10.1179/2045772313Y.0000000149

Huang H, He J, Herman R, Carhart MR (2006) Modulation effects of epidural spinal cord stimulation on muscle activities during walking. IEEE Trans Neural Syst Rehabil Eng 14:14–23

Hubli M, Dietz V, Schrafl-Altermatt M, Bolliger M (2013) Modulation of spinal neuronal excitability by spinal direct currents and locomotion after spinal cord injury. Clin Neurophysiol 124:1187–1195

Jilge B, Minassian K, Rattay F, Pinter MM, Gerstenbrand F, Binder H, Dimitrijevic MR (2004) Initiating extension of the lower limbs in subjects with complete spinal cord injury by epidural lumbar cord stimulation. Exp Brain Res 154:308–326

Kitano K, Koceja DM (2009) Spinal reflex in human lower leg muscles evoked by transcutaneous spinal cord stimulation. J Neurosci Methods 180:111–115

Krause P, Edrich T, Straube A (2004) Lumbar repetitive magnetic stimulation reduces spastic tone increase of the lower limbs. Spinal Cord 42:67–72

Ladenbauer J, Minassian K, Hofstoetter US, Dimitrijevic MR, Rattay F (2010) Stimulation of the human lumbar spinal cord with implanted and surface electrodes: a computer simulation study. IEEE Trans Neural Syst Rehabil Eng 18:637–645

Lin V, Hsiao I (2005) Clinical applications of functional magnetic stimulation in patients with spinal cord injuries. In: Hallett M, Chokroverty S (eds) Magnetic stimulation in clinical neurophysiology, 2nd edn. Elsevier, Philadelphia, pp 393–410

Maccabee PJ, Amassian VE, Eberle LP, Rudell AP, Cracco RQ, Lai KS, Somasundarum M (1991) Measurement of the electric field induced into inhomogeneous volume conductors by magnetic coils: application to human spinal neurogeometry. Electroencephalogr Clin Neurophysiol 81:224–237

Maccabee PJ, Lipitz ME, Desudchit T, Golub RW, Nitti VW, Bania JP, Willer JA, Cracco RQ, Cadwell J, Hotson GC, Eberle LP, Amassian VE (1996) A new method using neuromagnetic stimulation to measure conduction time within the cauda equina. Electroencephalogr Clin Neurophysiol 101:153–166

Maccabee PJ, Eberle LP, Stein IA, Willer JA, Lipitz ME, Kula RW, Marx T, Muntean EV, Amassian VE (2011) Upper leg conduction time distinguishes demyelinating neuropathies. Muscle Nerve 43:518–530

Martin PG, Butler JE, Gandevia SC, Taylor JL (2008) Noninvasive stimulation of human corticospinal axons innervating leg muscles. J Neurophysiol 100:1080–1086

Matsumoto H, Octaviana F, Hanajima R, Terao Y, Yugeta A, Hamada M, Inomata-Terada S, Nakatani-Enomoto S, Tsuji S, Ugawa Y (2009a) Magnetic lumbosacral motor root stimulation with a flat, large round coil. Clin Neurophysiol 120:770–775

Matsumoto H, Octaviana F, Terao Y, Hanajima R, Yugeta A, Hamada M, Inomata-Terada S, Nakatani-Enomoto S, Tsuji S, Ugawa Y (2009b) Magnetic stimulation of the cauda equina in the spinal canal with a flat, large round coil. J Neurol Sci 284:46–51

Mills KR, Murray NM (1986) Electrical stimulation over the human vertebral column: which neural elements are excited? Electroencephalogr Clin Neurophysiol 63:582–589

DOI 10.1007/978-1-4614-7320-6_603-6

Mills KR, McLeod C, Sheffy J, Loh L (1993) The optimal current direction for excitation of human cervical motor roots with a double coil magnetic stimulator. Electroencephalogr Clin Neurophysiol 89:138–144

Minassian K, Jilge B, Rattay F, Pinter MM, Binder H, Gerstenbrand F, Dimitrijevic MR (2004) Stepping-like movements in humans with complete spinal cord injury induced by epidural stimulation of the lumbar cord: electromyographic study of compound muscle action potentials. Spinal Cord 42:401–416

Minassian K, Persy I, Rattay F, Dimitrijevic MR, Hofer C, Kern H (2007) Posterior root-muscle reflexes elicited by transcutaneous stimulation of the human lumbosacral cord. Muscle Nerve 35:327–336

Minassian K, Hofstoetter US, Rattay F (2011) Transcutaneous lumbar posterior root stimulation for motor control studies and modification of motor activity after spinal cord injury. In: Dimitrijevic MR, Kakulas BA, McKay WB, Vrbova G (eds) Restorative neurology of spinal cord injury. Oxford University Press, New York, pp 226–255

Minassian K, Hofstoetter U, Tansey K, Mayr W (2012) Neuromodulation of lower limb motor control in restorative neurology. Clin Neurol Neurosurg 114:489–497

Miranda PC (2005) Basic electromagnetism. In: Hallett M, Chokroverty S (eds) Magnetic stimulation in clinical neurophysiology, 2nd edn. Elsevier, Philadelphia, pp 1–15

Nielsen JF, Sinkjaer T (1997) Long-lasting depression of soleus motoneurons excitability following repetitive magnetic stimuli of the spinal cord in multiple sclerosis patients. Mult Scler 3:18–30

Pinter MM, Gerstenbrand F, Dimitrijevic MR (2000) Epidural electrical stimulation of posterior structures of the human lumbosacral cord: 3. Control of spasticity. Spinal Cord 38:524–531

Rattay F (1999) The basic mechanisms for the electrical stimulation of the nervous system. Neuroscience 89:335–346

Riehl M (2008) TMS stimulator design. In: Wassermann EM, Epstein CM, Ziemann U, Walsh V, Paus T, Lisanby SH (eds) The oxford handbook of transcranial stimulation. Oxford University Press, New York, pp 13–23

Rossini PM, Barker AT, Berardelli A, Caramia MD, Caruso G, Cracco RQ, Dimitrijević MR, Hallett M, Katayama Y, Lücking CH, de Noordhout AM, Marsden CD, Murray NM, Rothwell JC, Swash M, Tomberg C (1994) Non-invasive electrical and magnetic stimulation of the brain, spinal cord and roots: basic principles and procedures for routine clinical application. Report of an IFCN committee. Electroencephalogr Clin Neurophysiol 91:79–92

Roy FD, Gibson G, Stein RB (2012) Effect of percutaneous stimulation at different spinal levels on the activation of sensory and motor roots. Exp Brain Res 223:281–289

Sandbrink F (2008) The MEP in clinical neurodiagnosis. In: Wassermann EM, Epstein CM, Ziemann U, Walsh V, Paus T, Lisanby SH (eds) The Oxford handbook of transcranial stimulation. Oxford University Press, New York, pp 237–283

Sommer M (2008) TMS waveform and current direction. In: Wassermann EM, Epstein CM, Ziemann U, Walsh V, Paus T, Lisanby SH (eds) The Oxford handbook of transcranial stimulation. Oxford University Press, New York, pp 7–12

Szava Z, Danner SM, Minassian K (2011) Transcutaneous electrical spinal cord stimulation: biophysics of a new rehabilitation method after spinal cord injury. VDM Verlag Dr. Müller, Saarbrücken

Taylor JL, Gandevia SC (2004) Noninvasive stimulation of the human corticospinal tract. J Appl Physiol 96:1496–1503

Troni W, Bianco C, Coletti Moja M, Dotta M (1996) Improved methodology for lumbosacral nerve root stimulation. Muscle Nerve 19:595–604

DOI 10.1007/978-1-4614-7320-6_603-6

Troni W, Di Sapio A, Berra E, Duca S, Merola A, Sperli F, Bertolotto A (2011) A methodological reappraisal of non invasive high voltage electrical stimulation of lumbosacral nerve roots. Clin Neurophysiol 122:2071–2080

Troni W, Benech CA, Perez R, Tealdi S, Berardino M, Benech F (2013) Non-invasive high voltage electrical stimulation as a monitoring tool of nerve root function in lumbosacral surgery. Clin Neurophysiol 124:809–818

Ugawa Y, Rothwell JC, Day BL, Thompson PD, Marsden CD (1989) Magnetic stimulation over the spinal enlargements. J Neurol Neurosurg Psychiatry 52:1025–1032

Xia Q, Wang S, Passias PG, Kozanek M, Li G, Grottkau BE, Wood KB, Li G (2009) In vivo range of motion of the lumbar spinous processes. Eur Spine J 18:1355–1362

Zidar J (2001) Are segmental conduction studies of the corticospinal tract in humans feasible? In: Proceedings of the international federation for medical & biological engineering. IFMBE Proceedings, Pula, pp 74–77